

Sonochemical Processes and Formation of Gold Nanoparticles within Pores of Mesoporous Silica

Wei Chen,^{*,†,1} Weiping Cai,^{*} Liang Zhang,[†] Guozhong Wang,^{*} and Lide Zhang^{*}

^{*}Laboratory of Internal friction and Detects in Solids, Institute of Solid State Physics, Chinese Academy of Sciences, Hefei, Anhui 230031, People's Republic of China; and [†]Institute of Economy and Technology, University of Science and Technology of China, Hefei, Anhui 230026, People's Republic of China

E-mail: chewyff@mail.hf.ah.cn

Received September 27, 2000; accepted March 5, 2001

Mesoporous silica with gold nanoparticles inside its pores was prepared by the soaking and ultrasound-induced reduction method. This new composite was characterized by X-ray diffraction (XRD), Brunauer–Emmett–Teller (BET), and high-resolution transmission electron microscopy (HRTEM) techniques. The results showed that nearly spherical-shaped gold nanoparticles, with mean size in diameter of 5.2 nm, are located in the pores, most of which are less than 6 nm in diameter. The ultrasonic irradiation time dependence of optical absorption for the soaked porous solid sample, as suggested by the variation in absorbance at 310 and 544 nm, indicated the reduction of Au (III) ions, and the nucleation and aggregation of gold nanoparticles within pores of mesoporous silica. Additionally, the reaction rates estimated phenomenologically by the absorbance decay at 310 nm for both the porous sample and the corresponding soaking solution presented the enhancement of the sonochemical reduction rate of Au (III) ions within pores of mesoporous silica. It is assumed that the extensive liquid–solid interfacial zones in the pores, due to the high specific surface areas and great porosity of the mesoporous solid, are the major regions where the efficient sonochemical reduction induced by the cavitation takes place.

© 2001 Academic Press

Key Words: sonochemical reduction; gold nanoparticles; mesoporous silica; cavitation; liquid–solid interface.

I. INTRODUCTION

Nano-sized noble metal particles, because of their surface and quantum-size effects, display many novel properties (1, 2), such as high catalytic activities, interesting optical properties, and various properties from a fundamental viewpoint. Accordingly, considerable effort has been focused on the development of synthetic techniques. Many studies on the methods for their preparation were reported, such as controlled chemical reduction (3, 4), photochemical or radiation-chemical reduction (5, 6), and gas evaporation (7). In order to prevent the formation of undesired agglomeration, these processes are often performed in the presence of stabilizing ligands, polymers, or various surfactants. The stability of metallic colloids depends on the characteristics of the special protecting agents, which are generally stripped off from the metal surface in vacuum and/or with heating, result-

ing in agglomeration. Thus for application, the common way of immobilizing the metallic particles is to prepare them in the presence of a neutral solid support, which improves the nanoparticles stability.

Mesoporous solids, due to their large internal surface area and small pore size, have found great utility (8–10). Putting the nano-scaled particles (metals, semiconductors, or compounds) into the pores of mesoporous solids will form new composite materials. This material has received considerable attention in recent years because of its unique properties (11–13). It is, in structure and hence properties, significantly different from the recently extensively exported glass–metal colloid composite (films), organic–inorganic nanoparticles (films), or other nanocomposite films. The pores in this mesoporous composite are interconnected and open to ambient air; there inevitably exist both the interface between pore walls and particles and the free surface of the particles within pores, which is in contact with the ambience. This texture feature leads to many new physical and chemical effects, especially for metal particles, which are chemically active (2). For instance, in our previous work, the Ag/SiO₂ mesoporous composite displays optical switching and memory effects under different ambient conditions (14). Different techniques for promoting the formation of metal particles-loaded mesoporous composites have been developed. However, the formation of a metal/porous solid composite by assembling nanoparticles into the pores is often affected by the diffusion of the reducing gas or originally formed colloid, the interaction between solid support and metallic precursor, etc. The resultant properties of the materials are restricted by the wide size distribution of particles.

Extensive studies have reported that the sonochemical method could generate novel materials with unusual properties (15–19). The particles prepared in this way have a smaller size and a more narrow size distribution than those reported by other methods. The chemical effect of ultrasound is attributed to cavitation: formation, growth, and implosive collapse of bubbles, which lead to the decomposition of water molecules into hydrogen (H•) and hydroxyl (•OH) radicals owing to the production of high temperature and high pressure in collapsing cavities. Therefore, the preparation of fine particles of noble metals by application

of ultrasound appears to be an attractive possibility. Although noble metallic colloidal dispersions produced sonochemically from the corresponding aqueous solutions have been reported (16), to our knowledge, there have been few investigations on the formation of noble metallic nanoparticles within the pores of a mesoporous solid by ultrasonic irradiation. Recently we successfully synthesized a mesoporous solid with Au nanoparticles inside its pores by ultrasonic irradiation at room temperature. The subjects of the present report are the preparation of gold nanoparticles and the proposed sonochemical processes within the pores of mesoporous silica.

II. MATERIALS AND METHODS

Chloroauric acid ($\text{HAuCl}_4 \cdot 4\text{H}_2\text{O}$) (purity 99.9%) and analytical grade isopropanol were purchased commercially and used without further purification. The monolithic mesoporous silica host (planar-like, about 1 mm in thickness) was prepared by a sol-gel process from tetraethylorthosilicate (TEOS), drying, and finally annealing at 700°C for 1 h, as described in detail elsewhere (20). The BET technique (described in the following paragraph) shows that the measured value of specific surface area is 579 m^2/g and pore diameters fall in the range of 2–20 nm. The final porosity is estimated to be about 50%. Hence the silica prepared in this way is a typical mesoporous solid (8). Ultrasonic irradiation was accomplished with a KQ 218 sonication bath that was maintained at room temperature and operated at a frequency of approximately 40 kHz at 100-W output power. A Pyrex ground-in conical flask with cover (total volume ~ 100 mL) was used for the ultrasonic irradiation, which was carried out under an argon atmosphere.

A series of the preformed monolithic mesoporous silica host (parallel samples) was immersed in a 0.8 mmol L^{-1} HAuCl_4 solution (containing 0.2 mol L^{-1} isopropanol) for 3 weeks, which is long enough to make the concentrations of AuCl_4^- ions and isopropanol in the pores of the mesoporous silica be the same as those in bulk solution (21). After sufficient immersion, the solid samples with the corresponding mixed solution (about 50 ml) were transferred to the conical flask with cover, which was put in the sonication bath. The flask was purged with argon gas to eliminate any oxygen in it, before it was irradiated with 40-kHz ultrasonic waves at room temperature. During irradiation, a water flow was utilized to cool the glass vessel in the bath.

For the preparation of the Au/SiO₂ mesoporous composite, the immersed mesoporous solids were irradiated for 120 min and the whole sonication process was monitored at regular time intervals so that a parallel solid sample was taken out for optical absorption measurement after it was dried at 120°C for 30 min to remove the solvent (water) in the pores. The dried as-prepared composite was characterized by XRD, HRTEM, and BET techniques. For comparison, the corresponding soaking solution was irradiated simultaneously and the preformed silica hosts were also subjected to the same characterization.

Optical absorption spectra were measured at room temperature on a Cary 5E UV-VIS-NIR spectrophotometer over the wavelength range from 200 to 800 nm. The planar-like mesoporous composite was mounted vertically on a solid sample holder and the soaking solution irradiated simultaneously was transferred into a quartz sample cell 1 cm in length along the incident light. XRD examinations were carried out to examine the crystallinity of Au particles, which was recorded using an MXP 18 AHF, $\text{CuK}\alpha$ diffractometer. The pore structure of the irradiated sample was analyzed by N₂ sorption isotherm (at liquid N₂ temperature) on a gas adsorption apparatus (model: COULTER OMNISORP 100CX). Specific surface areas were evaluated using the BET equation (22), with data points between reduced pressure values of 0.05 and 0.25 and assuming the surface area occupied by one molecule was 16.2 Å. The measured error of specific surface area can be controlled to below 1.5%. For direct observation of Au particles in silica, the irradiated samples were first ground and dispersed in ethanol in a test tube. The latter was placed in a sonication bath for 10 min. The clear liquid from the top portion of the test tube was taken and a few drops were placed on a carbon-coated copper grid. After evaporation of acetone the copper grid was mounted on a JEOL 2010 high-resolution transmission electron microscope operated at 200 kV, and hence the microstructure was investigated.

III. RESULTS AND DISCUSSION

Characterization of Gold Nanoparticles within the Pores of Mesoporous Silica

It was observed by eye that the color of the composite samples, which were taken out at each irradiation time interval, changed gradually from yellow to pale purple and was quite transparent for optical measurements. The time dependence on optical absorption of the irradiated samples, as suggested by variance at peaks of 310 and 544 nm in Fig. 1, was associated with the

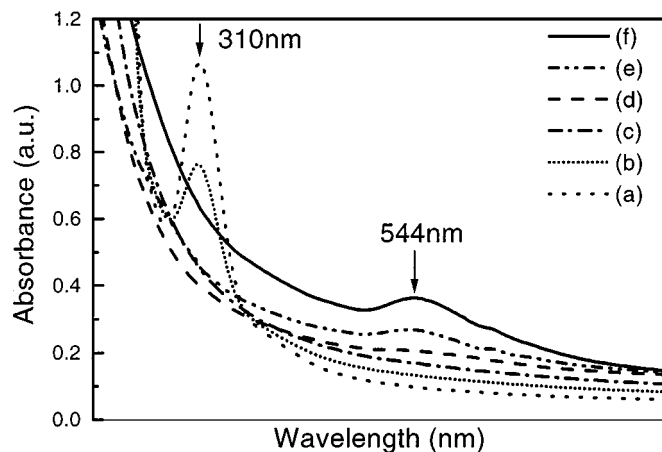


FIG. 1. Optical absorption spectra of the Au/SiO₂ mesoporous composite. Curves (a)–(f) refer to the spectra of the sample irradiated by ultrasound for 0, 10, 20, 40, 100, and 120 min respectively.

sonochemical reduction of AuCl_4^- ions, the aggregation of the reduced atoms, and the formation of Au nanoparticles within pores of the silica host. Before ultrasonic irradiation, curve (a) presents an absorption peak around 310 nm, indicating that the host contained only AuCl_4^- ions but no Au particle (23). During the irradiation, the peak around 310 nm decreased and disappeared in 20 min., demonstrating that the sonochemical reduction of AuCl_4^- ions had occurred. However, in the meantime, no apparent surface plasma resonance (SPR) absorption of Au particles appeared (24), which may be ascribed to the Au clusters with low nucleation. With the time increasing, the aggregation of the unstable Au oligomers can be revealed by the predominated SPR peak accompanied by its ever-decreasing bandwidth.

Figure 2 shows the absorption spectra of the corresponding soaking solution, which was irradiated by ultrasound simultaneously. In the surfactant-free solution, peaks at 220 and 310 nm ascribe to the intense charge transfer (CT) band and a moderate d-d transition band of HAuCl_4 (25). It was indicated that the SPR absorption of Au particles at 544 nm developed gradually during ultrasonic irradiation, while the specific peaks for AuCl_4^- decreased and disappeared in around 120 min. One can thus estimate qualitatively by the absorption decay at 310 nm that the rate of the reduction of Au (III) in bulk solution was much slower than that in the mesoporous solid (say, decay in 20 min.).

Figure 3 shows the XRD patterns of the as-prepared Au/SiO_2 mesoporous composite (i.e., after being irradiated by ultrasound for 120 min.) and the preformed silica host. XRD has confirmed, in addition to the amorphous silica pattern around $2\theta = 23^\circ$, the presence of the diffraction peaks corresponding to the (111), (200), (220), and (311) planes of cubic Au crystal.

Figure 4 shows the nitrogen sorption isotherms for the preformed silica host (reference sample) and the as-prepared Au/SiO_2 composite. It has been shown that the measured specific surface area decreases significantly from $579 \text{ m}^2/\text{g}$ for the

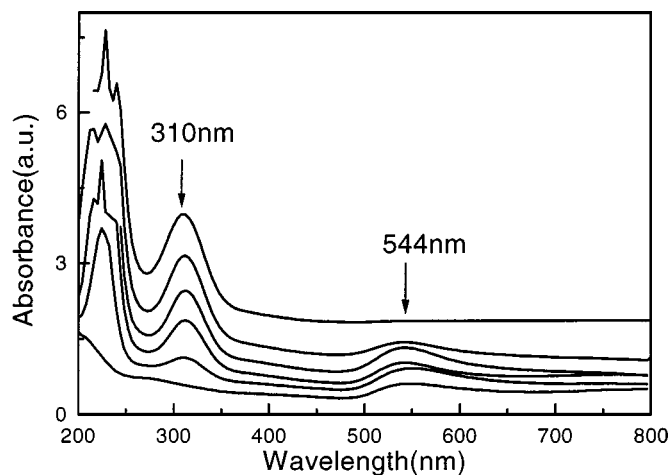


FIG. 2. Optical absorption spectra of the corresponding soaking solution. Curves from top to bottom refer to the spectra of the aqueous samples irradiated by ultrasound for 0, 40, 60, 80, 100, and 120 min respectively.

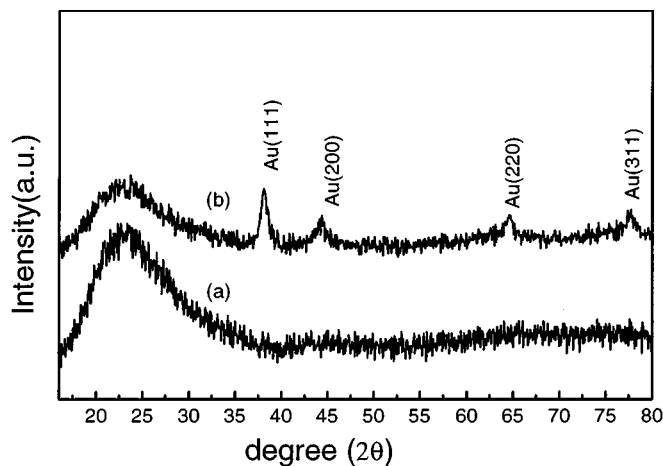


FIG. 3. X-ray diffraction patterns for the silica host (a) and the as-prepared Au/SiO_2 mesoporous composite (b).

reference sample to $535 \text{ m}^2/\text{g}$ for the as-prepared composite, although the real specific surface area may increase due to the existence of Au particles in the pores. This can be attributed to the presence of particles within the pores of silica, which leads to the difficulty of nitrogen molecules of going into too small free space during measurement, and hence partial areas cannot be measured (14). The presence of the particles within the pores is more clearly shown by the nitrogen sorption isotherms for both the reference and the loaded sample, as indicated in Fig. 4. The whole curve (b) for the as-prepared Au/SiO_2 composite is lower than curve (a) for the preformed silica host. Going further, analysis of the pore diameter, by the sorption apparatus with a computer attached, reveals that the pore diameter is sharply distributed around 5.7 nm and most pores (more than 90% in pore volume) are less than 5.9 nm in diameter, as shown in the inset of Fig. 4.

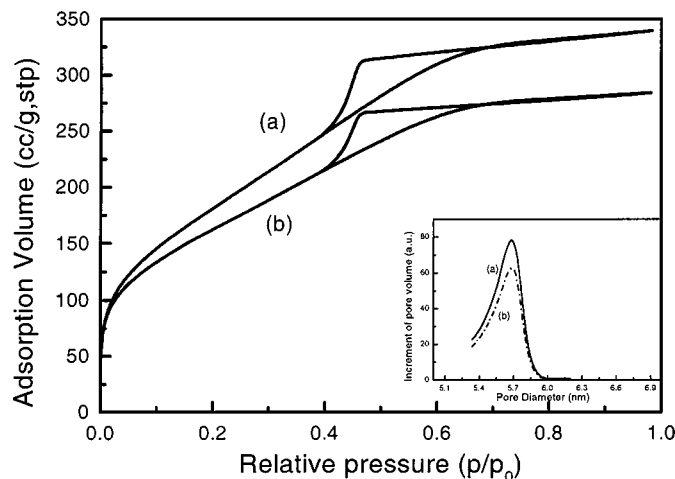


FIG. 4. Nitrogen sorption isotherms and pore size distributions of the silica host (a) and as-prepared Au/SiO_2 mesoporous composite (b).

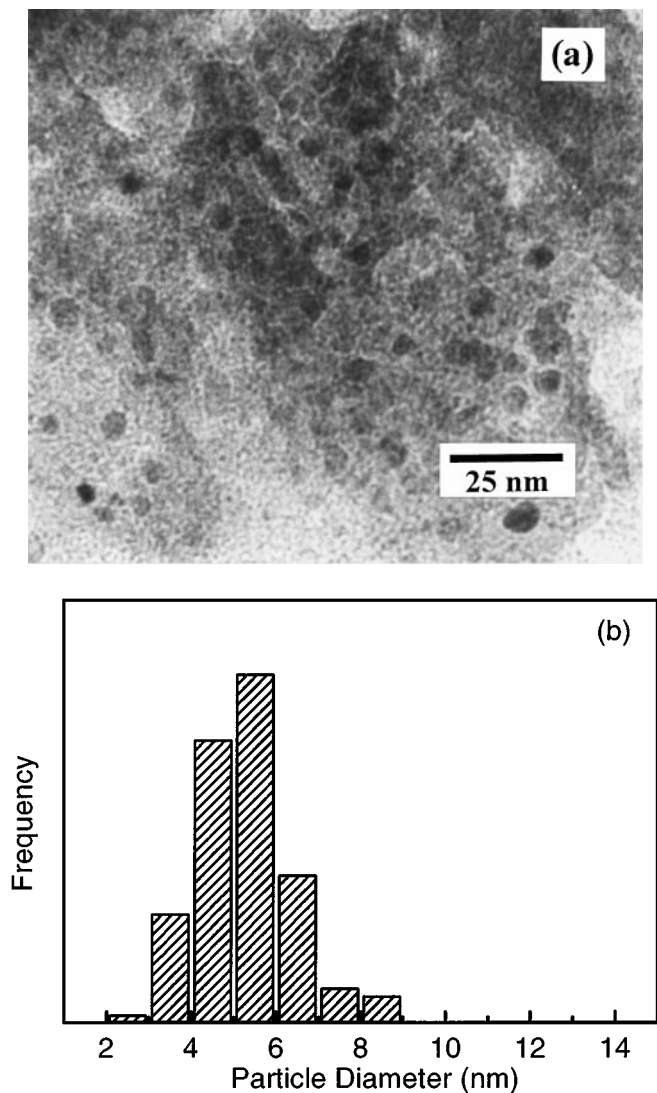


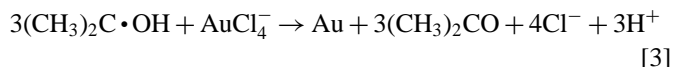
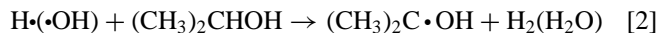
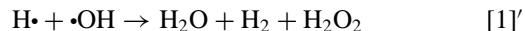
FIG. 5. (a) The morphology micrograph of the as-prepared Au/SiO₂ mesoporous composite. (b) Size distribution histogram of the gold particles within the pores of the mesoporous silica.

The HRTEM observation of the as-prepared Au/SiO₂ mesoporous composite is shown in Fig. 5a. It indicated that nearly spherical-shaped Au particles are dispersed uniformly in amorphous silica. The histogram of the particle sizes (Fig. 5b) exhibits a narrow size distribution with a mean particle diameter of 5.2 nm. Compared with the TEM observation for the soaking solution (not shown here) that the mean size of the Au nanoparticles was about 20–30 nm. Accompanied by the tendency to aggregate, the size-defined and stabilized Au nanoparticles in the solid sample were formed sonochemically within the confined space of the mesoporous silica, as discussed above.

Sonochemical Process for the Formation of Gold Nanoparticles in Mesoporous Silica

The chemical reactions driven by intense ultrasonic waves strong enough to produce cavitation are oxidation, reduction,

dissolution, and decomposition (15, 26). Nagata and co-workers (16) have proposed the mechanism of sonochemical reduction of AuCl₄⁻ ions and the formation of small Au particles in water. In the present study, for the mesoporous solid containing chloroauric acid, water, and alcohols after sufficient immersion, it is expected that the sonochemical reaction in it will show some character of that in liquid. Several processes within pores and in soaking solution are revealed to be involved, such as sonochemical reduction of Au (III) ions and the nucleation and aggregation of Au nanoparticles. During these processes, it is difficult for the Au oligomer or its larger aggregation to diffuse into pores of mesoporous silica. However, we cannot exclude the possibility of the exchange of AuCl₄⁻ ions from solution from inside the pores of silica, and the nucleation and aggregation into gold nanoparticles. The contribution may be small in limited time of ultrasonic irradiation (say, 120 min). Therefore the processes, such as reduction of AuCl₄⁻ ions inside pores of silica, and the nucleation and aggregation of gold particles, may be primarily responsible for the formation of small Au particles in pores. The expected reactions can be shown in



H \cdot and \cdot OH radicals originated due to thermal decomposition of H₂O with intense local heating and high pressures as shown in reaction [1]. Reaction [2] indicates the formation of strong reducing radicals (CH₃)₂C \cdot OH via hydrogen abstraction from the isopropanol by H \cdot and \cdot OH hydroxyl radicals. Multivalent AuCl₄⁻ ions in the pores were reduced rapidly by multistep radical reactions and subsequently the Au atoms aggregated, as shown in reactions [3] and [4].

What was unexpected was that the reduction of Au (III) ions in a porous solid was preceded more rapidly than that in soaking solution, as estimated in Fig. 1 and Fig. 2. It is known that the nucleation of bubbles in a liquid often occurs at less weak points, such as gas-filled crevices in suspended particulate matter or from transient microbubbles from a prior event (18). In the case of a mesoporous solid containing precursory solution, the large amount of liquid–solid interface in pores, due to the high specific surface areas and great porosity of mesoporous solid, where the tensile strength of solvent (water) was relatively weak, resulted in the easier formation and collapse of bubbles in the confined volume of pores with the present ultrasonic irradiation technique. Accordingly, the extensive liquid–solid interfacial zones in the pores are the major areas where the intensive sonochemical reaction induced by the cavitation takes place, and the Au (III) ions within the pores were reduced more efficiently.

To gain more knowledge about the mechanism of formation of gold nanoparticles, controlled experiments were carried out, i.e., the irradiation of the mixture of mesoporous silica and $0.8 \text{ mmol L}^{-1} \text{ HAuCl}_4$ soaking solution without any additive under the same sonochemical conditions. It was observed that the presence of isopropanol has a crucial influence on the sonochemical reduction rate of AuCl_4^- ions. Without the additive, $\text{H}\cdot$ and $\cdot\text{OH}$ radicals would readily recombine to give a variety of products as shown in reaction [1]' (27). Some other additives used in our investigation were also found to act as radical-scavenger and accelerator of the sonochemical reduction reaction. This gives support to the mechanism in which the reduction of Au ions proceeds via reaction [2] and [3] in the presence of an additive. Details about the dedication of these two reactions to the generation of reducing radicals in porous sonochemistry need further investigation.

In addition, the formation rate of gold nanoparticles in air decreased significantly compared with that under an argon atmosphere. One of the reasons may be the smaller cavitation effect in air than in argon due to the g value (C_p/C_v) of air (1.40) being lower than that of argon (1.67), where C_p and C_v are the constant pressure-specific heat and constant volume-specific heat of a medium, respectively. We presumed that the oxygen in air inhibited the reduction of gold ions by scavenging reducing radicals ($\text{R}\cdot$) as well as scavenging hydrogen atoms:



In summary, mesoporous silica with gold nanoparticles inside its pores was successfully synthesized by the soaking and ultrasonic irradiation method at room temperature. The optical absorption analyses combined with XRD, BET, and HRTEM techniques revealed that the intensive sonochemical reaction in the porous internal liquid–solid interfacial zones, due to the large amount of specific surface area and great porosity of mesoporous silica, resulted in the efficient reduction of Au (III) ions into Au atoms and aggregation into Au particles thereafter.

ACKNOWLEDGMENT

Support from the National Natural Science Foundation of China (10074065) is gratefully acknowledged.

REFERENCES

- Haperin, W. P., *Rev. Mod. Phys.* **58**, 533 (1986).
- Suryanarayana, C., *Int. Mater. Rev.* **40**, 41 (1995).
- Bronstein, L., Kramer, E., Berton, B., Burger, C., Förster, S., and Antonietti, M., *Chem. Mater.* **11**, 1402 (1999).
- Sato, S., Toda, K., and Oniki, S., *J. Colloid Interface Sci.* **218**, 504 (1999).
- Fukumi, K., Chayahara, A., Kadono, K., Sakaguchi, T., Horino, Y., Miya, M., Hayakawa, J., and Satou, M., *Jpn. J. Appl. Phys.* **28**, 742 (1991).
- Kurihara, K., Kizling, J., Stenius, P., and Fendler, J. H., *J. Am. Chem. Soc.* **105**, 2574 (1983).
- Satoh, N., and Kimura, K., *Bull. Chem. Soc. Jpn.* **62**, 1758 (1989).
- Hudson, M., and Sequeira, C. A., "Multifunctional Mesoporous Inorganic Solids." Kluwer, Dordrecht, 1993.
- Kresge, C. T., and Leonwicz, M. E., *Nature* **359**, 710 (1992).
- Monnier, A., *Science* **261**, 1299 (1993).
- Tanev, P. T., and Chibwe, M., *Nature* **368**, 321 (1994).
- Wu, C. G., and Thomas, B., *Science* **264**, 1758 (1994).
- Wilkinson, N. J., Alam, M. A., Clayton, J. M., Evans, R., Fretwell, H. M., and Usmar, S. G., *Phys. Rev. Lett.* **69**, 3535 (1992).
- Cai, W., Tan, M., Wang, G., and Zhang, L., *Appl. Phys. Lett.* **69**, 2980 (1996).
- Suslick, K. S., "Ultrasound: Its Chemical Physical and Biological Effects." VCH, Weinheim, 1988.
- Okitsu, K., Mizukoshi, Y., Bandow, H., Maeda, Y., Yamamoto, T., and Nagata, Y., *Ultrason. Sonochem.* **3**, S249 (1996).
- Arul Dhas, N., Zaban, A., and Gedanken, A., *Chem. Mater.* **11**, 806 (1999).
- Suslick, K. S., *Science* **247**, 1439 (1990).
- Hyeon, T., Fang, M., and Suslick, K. S., *J. Am. Chem. Soc.* **118**, 5492 (1996).
- Cai, W., and Zhang, L., *J. Phys.: Condens. Matter* **9**, 7257 (1997).
- Koone, N. D., and Zerda, T. W., *J. Non-Cryst. Solids* **183**, 243 (1995).
- Brunauer, S., Emmett, P. H., and Teller, E., *J. Am. Chem. Soc.* **60**, 309 (1938).
- Khlebtsov, N. G., Bogatyrev, V. A., Dykman, L. A., and Melnikov, A. G., *J. Colloid Interface Sci.* **180**, 436 (1996).
- Creighton, J. A., and Eadon, D. G., *J. Chem. Soc. Faraday Trans.* **37**, 3537 (1991).
- Esumi, K., Hara, J., Aihara, A., Usui, K., and Torigoe, K., *J. Colloid Interface Sci.* **208**, 578 (1998).
- Hayes, D., Micic, O. L., Nenadovic, M. T., Swayambunathan, V., and Meisel, D., *J. Phys. Chem.* **93**, 4603 (1989).
- Gutierrez, M., Henglein, A., and Dohrmann, J., *J. Phys. Chem.* **91**, 6687 (1987).